JACS
JOURNAL OF THE AMERICAN CHEMICAL SOCIETY
pubs.acs.org/JACS
Article

Expanded Helicenes as Synthons for Chiral Macrocyclic Nanocarbons

Gavin R. Kiel, Katherine L. Bay, Adrian E. Samkian, Nathaniel J. Schuster, Janice B. Lin, Rex C. Handford, Colin Nuckolls, K. N. Houk, and T. Don Tilley*

Cite This: J. Am. Chem. Soc. 2020, 142, 11084–11091
Read Online

ABSTRACT: Expanded helicenes are large, structurally flexible π-frameworks that can be viewed as building blocks for more complex chiral nanocarbons. Here we report a gram-scale synthesis of an alkyne-functionalized expanded [11]helicene and its single-step transformation into two structurally and functionally distinct types of macrocyclic derivatives: (1) a figure-eight dimer via alkyne metathesis (also gram scale) and (2) two arylene-bridged expanded helicenes via Zr-mediated, formal [2+2+*n*] cycloadditions. The phenylene-bridged helicene displays a substantially higher enantiomerization barrier (22.1 kcal/mol) than its helicene precursor (<11.9 kcal/mol), which makes this a promising strategy to access configurationally stable expanded helicenes. In contrast, the topologically distinct figure-eight retains the configurational lability of the helicene precursor. Despite its lability in solution, this compound forms homochiral single crystals. Here, the configuration is stabilized by an intricate network of two distinct yet interconnected helical superstructures. The enantiomerization mechanisms for all new compounds were probed using density functional theory, providing insight into the flexibility of the figure-eight and guidance for future synthetic modifications in pursuit of non-racemic macrocycles.

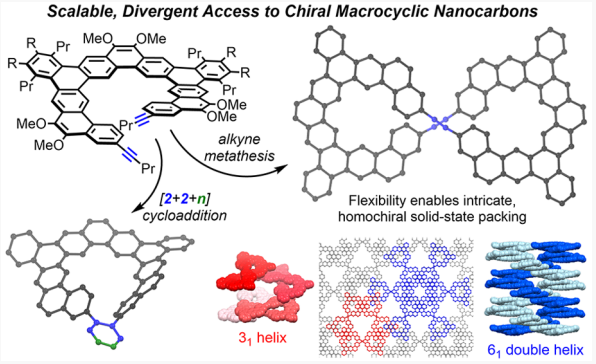

INTRODUCTION

There is a rapidly growing appreciation that chirality endows conjugated nanocarbons and related polycyclic aromatic hydrocarbons (PAHs) with novel photophysical ("chiroptical"), electronic, and supramolecular properties.[1] Thus, chirality is an orthogonal design element for diverse applications in molecular nanotechnology (e.g., machines and switches) and organic electronics.[2] Chiral nanocarbons occupy a vast chemical space, and tremendous effort has been devoted to their synthesis and evaluation.[1−3] Constraining a nanocarbon into a macrocyclic framework is a common way to introduce chirality into an otherwise achiral structure, and might provide a means to increase the configurational stability in those that are inherently chiral.[4] More importantly, new properties can emerge in a macrocyclic environment as a result of its impact on molecular topology and spatial orientation of constituent units.[4,5]

As the prototypical chiral PAHs, carbohelicenes (**A**, Figure 1a) are natural building blocks for more complex chiral nanocarbons. Fusion of more than one helicene into a contiguous PAH framework gives rise to "multiple helicenes" (e.g., **B**),[6] which exhibit unique solid-state behavior as a result of their contorted[6b] structures (e.g., formation of host−guest complexes with acceptor molecules[6d] and π-stacking in three dimensions[6e]). Introduction of helicenes into "non-fused" oligomeric or polymeric structures (i.e., where they are not part of the same PAH framework) has also yielded interesting results.[7] For example, Di Bari and Diedrich demonstrated that photophysical and chiroptical properties can be significantly enhanced in an oligomeric structure[7a] and Yamaguchi has developed numerous helicene oligomers (e.g., **C**) that exhibit a range of complex self-assembly phenomena.[7b,c] Notably, many of these self-assembling oligomers are macrocyclic. Other helicene-containing macrocycles possess fascinating molecular topologies.[7d−j] Along these lines, a few groups isolated figure-eight dimers constructed from [5]helicenes (e.g., **D**) or their heterocyclic analogues[7d−f] and Isobe synthesized an analogous dimer of [4]helicene (**E**), which is a molecular manifestation of Penrose's illusory never-ending staircase.[7g] Finally, there have been two instances of macrocyclic [5]helicene trimers that display Möbius topology. Durola and Herges reported D_3-symmetrical trimer **F**,[7h] for which a rare "triply-twisted" topology gives rise to Möbius aromaticity (the C_2 isomer was

Received: March 23, 2020
Published: May 26, 2020

https://dx.doi.org/10.1021/jacs.0c03177
J. Am. Chem. Soc. 2020, 142, 11084−11091

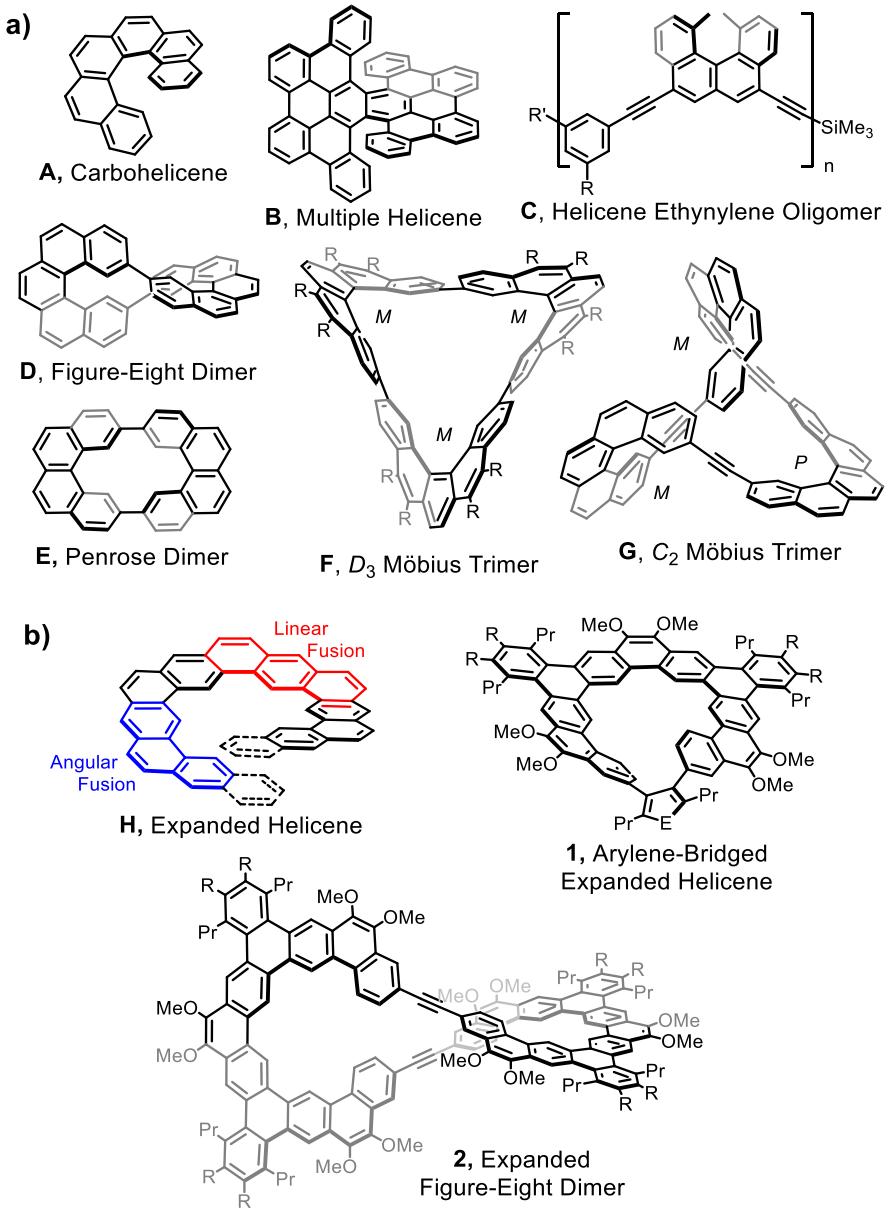

Figure 1. (a) Examples of chiral nanocarbons derived from carbohelicene building blocks. (b) New chiral macrocyclic nanocarbons (**1** and **2**) derived from an expanded helicene (this work).

also isolated). While the current manuscript was under review, Moore, Zhu, and Garcia-Garibay reported trimer **G**,[7i] which differs from **F** based on its ethynyl spacers and C_2 symmetry.

In 2017, the Tilley group introduced a new class of chiral nanocarbons, the "expanded helicenes" (**H**, Figure 1b), which have larger cavities and diameters than **A** as a result of alternating angular and linear ring-fusion.[8] With the aid of a general, [2+2+*n*] cycloaddition strategy, these compounds were shown to exhibit unique self-assembly (e.g., a π-stacked double helix) and low enantiomerization free energy barriers ($\Delta G^{\ddagger}_{enant}$), both resulting from their conformationally flexible backbones. Such flexibility was more recently observed and studied computationally for an unsubstituted example by Matsuda and co-workers.[9] These authors also suggested that this class of molecules will possess exceptional chiroptical properties (e.g., strong excitation dissymmetry factors) as a result of their larger diameters, but this has not yet been experimentally validated due to their low $\Delta G^{\ddagger}_{enant}$ values. Thus, strategies to increase $\Delta G^{\ddagger}_{enant}$ are of significant interest.

This contribution describes a scalable and divergent synthetic route to two structurally and functionally distinct chiral macrocyclic nanocarbons (**1** and **2**, Figure 1b) from a single expanded helicene building block. The first, a geometrically constrained "arylene-bridged" expanded helicene (**1**), provides an effective platform to increase configurational stability, which is an important step toward interrogation of expanded helicene chiroptical properties. The second, a topologically distinct figure-eight arylene ethynylene macrocycle (**2**), retains the flexibility and conformational lability of its helicene precursor, which appears to facilitate its unique crystal packing. An important step toward accessing **1** and **2** was development of a simple, gram-scale synthesis of the helicene precursor **3** (Scheme 1), which contains alkynyl groups at its termini. This was enabled by application of a recently discovered,[10] site-selective [2+2+2] reaction. The

https://dx.doi.org/10.1021/jacs.0c03177
J. Am. Chem. Soc. 2020, 142, 11084−11091

Scheme 1. Gram-Scale Synthesis of Alkynylated Expanded [11]Helicene 3

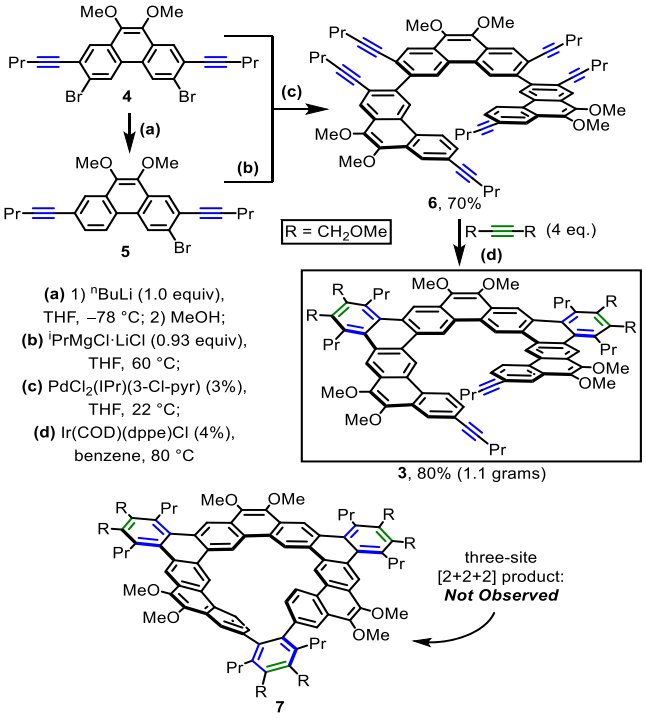

preserved alkynyl groups at the termini of **3** undergo a formal [2+2+*n*] cycloaddition (two examples) and alkyne metathesis to give **1** and **2**, respectively (Scheme 2). Importantly, the orthogonality of these transformations makes them amenable to a rapid, one-pot process.

RESULTS AND DISCUSSION

The synthesis of alkynylated expanded helicene **3** (Scheme 1) was accomplished in three steps from phenanthrene dibromide **4**. The previously reported procedure[8] for **4** proved to be highly scalable, providing routine access to 35−40 g of this compound. Treatment of **4** with 1.0 equiv of ^{n}BuLi resulted in a selective monolithiation via lithium−bromine exchange, giving **5** after a MeOH quench.[10] The reaction of **5** with ^{i}PrMgCl·LiCl gave an *in situ*-generated Grignard reagent that was Kumada cross-coupled with **4** to give hexa(alkynyl)-terphenanthrene **6** in 70% yield. Subjection of **6** to the previously developed,[8,10,11] Ir-catalyzed [2+2+2] cycloaddition conditions afforded the desired helicene **3** in excellent yield (isolated: 80%; ^{1}H NMR: 88%). Notably, high dilution is not necessary for preservation of the reactive alkynyl groups (100 mM diyne concentration), which enabled the synthesis of **3** on a gram scale. Furthermore, helicene **3** was stable even when it was re-subjected (after isolation) to more forcing [2+2+2] conditions (10 equiv monoyne, 12% Ir(COD)(dppe)Cl, 105 °C in toluene-d_8), and the three-site [2+2+2] product (**7**) was not observed.

Scheme 2. Divergent Macrocyclization of Helicene 3 to Form Arylene-Bridged Helicenes 1 and Figure-Eight Dimer 2

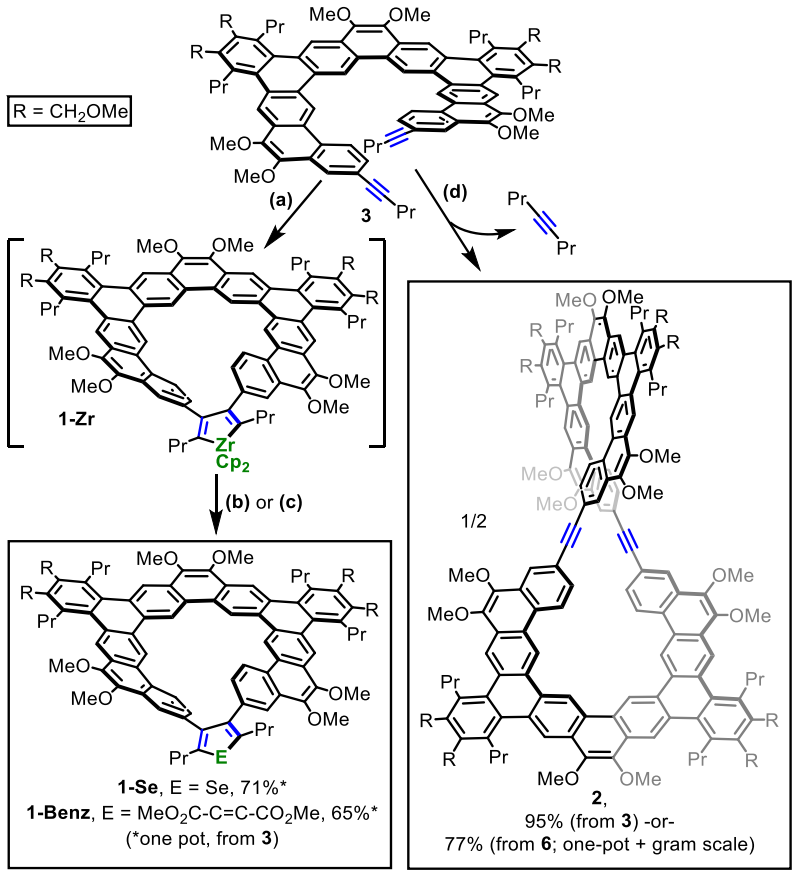

https://dx.doi.org/10.1021/jacs.0c03177
J. Am. Chem. Soc. 2020, 142, 11084−11091

The spatial orientation of the alkynyl groups in **3** suggested the possibility of a formal [2+2+*n*] cycloaddition to form the conformationally restricted, "bridged-helicene" structure **1** (Scheme 2).[12] Since the analogous **7** did not form under Ir catalysis (see above), we turned to a more reactive, low-valent zirconocene reagent. Upon treatment of a solution of helicene **3** in benzene-d_6 with 1.2 equiv of $Cp_2Zr(pyr)(Me_3SiC{\equiv}CSiMe_3)$,[13] the intermediate zirconacyclopentadiene-bridged helicene **1-Zr** was observed in 86% yield by ^{1}H NMR spectroscopy. Zirconacyclopentadienes are typically isolable, but they are most conveniently generated *in situ* as synthetic intermediates. Treatment of *in situ* generated **1-Zr** with $SeCl_2(bipy)$[8] or DMAD[14] (the latter after transmetalation to Cu) afforded **1-Se** or **1-Benz** in 71 and 65% yields, respectively. It is important to note that, due to synthetic versatility of zirconacyclopentadiene intermediates,[15] many divergent functionalizations of this type should be possible.

Alkyne metathesis is effective for the scalable, high-yielding synthesis of arylene ethynylene macrocycles,[16] which was recently exploited by the Tilley group for general incorporation of PAHs into such structures.[10] The two alkynyl groups at the termini of helicene **3** are suitably oriented to form the figure-eight macrocycle **2** (Scheme 2). Compound **2** was isolated in excellent yield (95%) after treatment of **3** with a 10% loading of $EtC{\equiv}Mo(OC(CH_3)(CF_3)_2)_3(DME)$[17] for 16 h at 80 °C, in the presence of powdered 5 Å molecular sieves (MS).[18] Purification required only a simple elution of the reaction mixture through silica gel. As previously observed,[10] 5 Å MS were effective for removal of the 4-octyne byproduct (see Figure S7), which drove the reaction to completion. Notably, the metathesis reaction proceeded to ~95% conversion without removal of 4-octyne (i.e., with no 5 Å MS), but this required careful chromatography to remove unreacted **3**. The identity of **2** was unambiguously determined by ^{1}H and ^{13}C NMR spectroscopies (the former displayed an absence of propargylic methylene resonances and the latter only one alkynyl resonance), MALDI-TOF, and single-crystal X-ray diffraction (Figure 2). Moore and co-workers recently reported an analogous macrocyclization of 2,13-dipropynyl[5]helicene via alkyne metathesis, which provides an interesting comparison.[7i] There, instead of a figure-eight dimer, helicene ethynylene trimer **G** (Figure 1a) was isolated as the sole product.

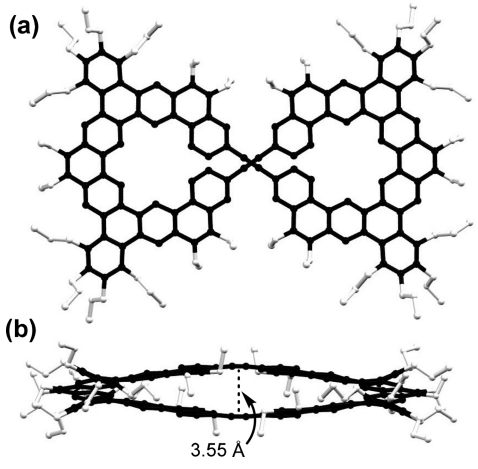

Figure 2. Molecular structure of **2** as determined by single-crystal X-ray diffraction: (a) top view and (b) side view.

Both types of macrocycles can also be accessed in a one-pot procedure from hexayne **6**, as demonstrated by the synthesis of **1-Benz** and **2** in 51 and 77% yields, respectively. These yields are comparable to those from the two-step procedures outlined above. *Furthermore, 1.2 g of the figure-eight macrocycle (**2**) was isolated using this one-pot approach.*

The new compounds are highly soluble in common aromatic and chlorinated solvents and insoluble in more polar and non-polar solvents. The ^{1}H NMR chemical shifts of **1-Se**, **2**, and **3** in chloroform-*d* are independent of concentration (see Figures S13−S15), suggesting that their high solubility results from limited aggregation via π-stacking in this solvent. In contrast, **1-Benz** appears to aggregate in chloroform-*d*, as evidenced by the moderate shielding of its aromatic resonances upon concentration (see Figure S12).

Single crystals of **2** were grown by slow evaporation of a CH_2Cl_2/hexanes solution, and the solid-state structure was elucidated by single-crystal X-ray diffraction (Figure 2). Like the previously reported figure-eight dimers of [5]helicene,[7d,e] compound **2** displays *PP*/*MM* helicity (i.e., the constituent helicenes are homochiral). This is also the lowest energy conformation in the gas-phase, as predicted by density functional theory (DFT) at the B3LYP-D3/6-31G(d) level of theory (Figure S39).

Compound **2** crystallizes in the uncommon, non-centrosymmetric space group $P6_422$, wherein each molecule of **2** is homochiral (Figure 3).[19] The remarkable solid-state packing

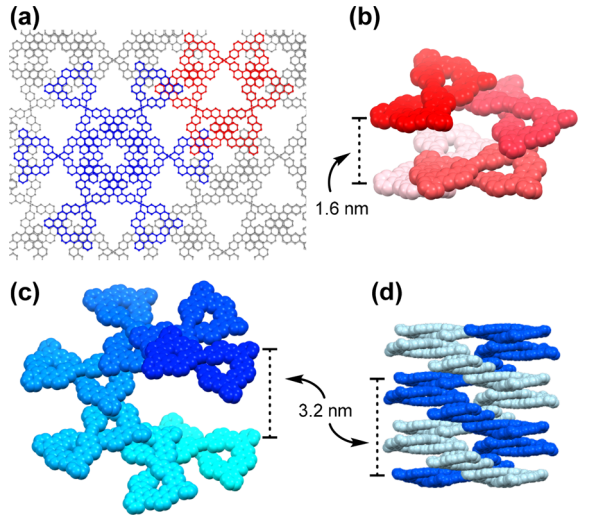

Figure 3. Solid-state packing of **2** as determined by single-crystal X-ray diffraction (side chains and solvent molecules are omitted for clarity).[19] (a) View along the crystallographic *c*-axis depicting the 3_1 (red) and 6_1 (blue) helical axes. Perspective view of a single turn of the (b) 3_1 and (c) 6_1 helices. (d) Double helical superstructure formed by two equivalent 6_1 helices.

features two parallel, interconnected helical axes (Figure 3a), containing three and six molecules of **2** per helical turn (Figure 3b,c). Here these are referred to as the 3_1 and 6_1 helices, respectively, based on the symbol of the screw axis of symmetry that relates their constituent molecules. The pitches of these supramolecular helices are 1.6 and 3.2 nm, respectively, and they are of opposite handedness. The large pitch of the latter serves to accommodate a symmetry-equivalent 6_1 partner, which gives rise to a double helical superstructure (Figure 3d). Each molecule of **2** engages in π-

https://dx.doi.org/10.1021/jacs.0c03177
J. Am. Chem. Soc. 2020, 142, 11084−11091

stacking interactions with *eight* neighboring molecules, with a shortest π-stacking distance of 3.5 Å. The pores are occupied by solvent molecules, which are highly disordered and were accounted for with the SQUEEZE[20] program. The notable differences in the X-ray and DFT-calculated molecular structures (see Figure S31 and the associated discussion), and the apparently small energy cost associated with the required conformational distortion, suggest that the flexibility of **2** plays an important role in its unique crystal packing.

The basic photophysical properties of the helicene system are not significantly perturbed by either type of macrocyclization, which likely results from the highly benzenoid[21] nature of these compounds. Although the expected redshift in absorption maximum (λ_{max}) is observed upon dimerization of **3** to form **2**, it is small (12 nm, from 322 to 334 nm; see Figure S29). The λ_{max} values for **1-Se**, **1-Benz**, and **3** are nearly identical (319−322 nm). The new compounds possess relatively large optical HOMO−LUMO gaps in the range of 2.9−3.0 eV, the magnitude of which is typical[21] for benzenoid PAHs. Likewise, the emission maxima (λ_{max}) are essentially unchanged (see Figure S30), each lying within 4 nm of the λ_{max} for **3** (448 nm).

The chirality of the new compounds results from their C_2 (for **1-Benz**, **1-Se**, and **3**) and D_2 (for **2**) symmetries. Their enantiomerization barriers ($\Delta G^{\ddagger}_{enant}$) were first probed via variable-temperature ^{1}H NMR spectroscopy, which was facilitated by the presence of diastereotopic methylene protons on the peripheral methoxymethyl groups. For the figure-eight dimer (**2**) and helicene (**3**), these measurements were complicated by aggregation at low temperatures (see Figures S19−S22). Nevertheless, ruling out accidental overlap of chemical shifts, upper bounds of 12.5 and 11.9 kcal/mol were estimated for **2** and **3**, respectively (based on the absence of singlet decoalescence in three solvents at low temperatures; see SI for further details on all enantiomerization experiments). Thus, **2** retains the configurational lability of its synthetic precursor, **3**. Due to conformational restrictions enforced by their bridging arylene rings, **1-Se** and **1-Benz** exhibit higher barriers. Surprisingly, however, the increase for **1-Se** was only moderate ($\Delta G^{\ddagger}_{enant}$ = 16.6 ± 0.3 kcal/mol at 65 °C), as determined by ^{1}H NMR spectroscopy in toluene-d_8 (Figure S17). For **1-Benz**, the absence of coalescence of its methylene doublets up to 130 °C in mesitylene (Figure S18) provided only a lower bound for $\Delta G^{\ddagger}_{enant}$ of >20 kcal/mol.

The higher $\Delta G^{\ddagger}_{enant}$ for **1-Benz** motivated attempts to resolve its enantiomers by chiral high-performance liquid chromatography (HPLC). The enantiomers separated readily at 25 °C (Figure S23), but their interconversion at room temperature prevented the isolation of an enantiopure sample. A $\Delta G^{\ddagger}_{enant}$ of 22.1 ± 0.1 kcal/mol and racemization half-life of 16 min (both at 25 °C) in toluene were determined by measurement of the decay in circular dichroism of an enantioenriched sample (Figures S25−S28). Resolution of **1-Se**, **2**, or **3** was not attempted using chiral HPLC due to their low $\Delta G^{\ddagger}_{enant}$. In principle, the spontaneous resolution of **2** in the solid state (see above) should enable a measurement of its chiroptical properties if the conglomerates[19] could be manually separated; however, its low $\Delta G^{\ddagger}_{enant}$ complicates the possibility of a solution measurement.

To guide the future design of macrocycles with higher $\Delta G^{\ddagger}_{enant}$ and to provide insight into the structural flexibility of **2**, the enantiomerization mechanisms of the new compounds were probed computationally by DFT at the B3LYP-D3/6-31G(d) level of theory. The calculated (gas-phase) transition states and associated $\Delta G^{\ddagger}_{enant}$ values are shown in Figure 4,

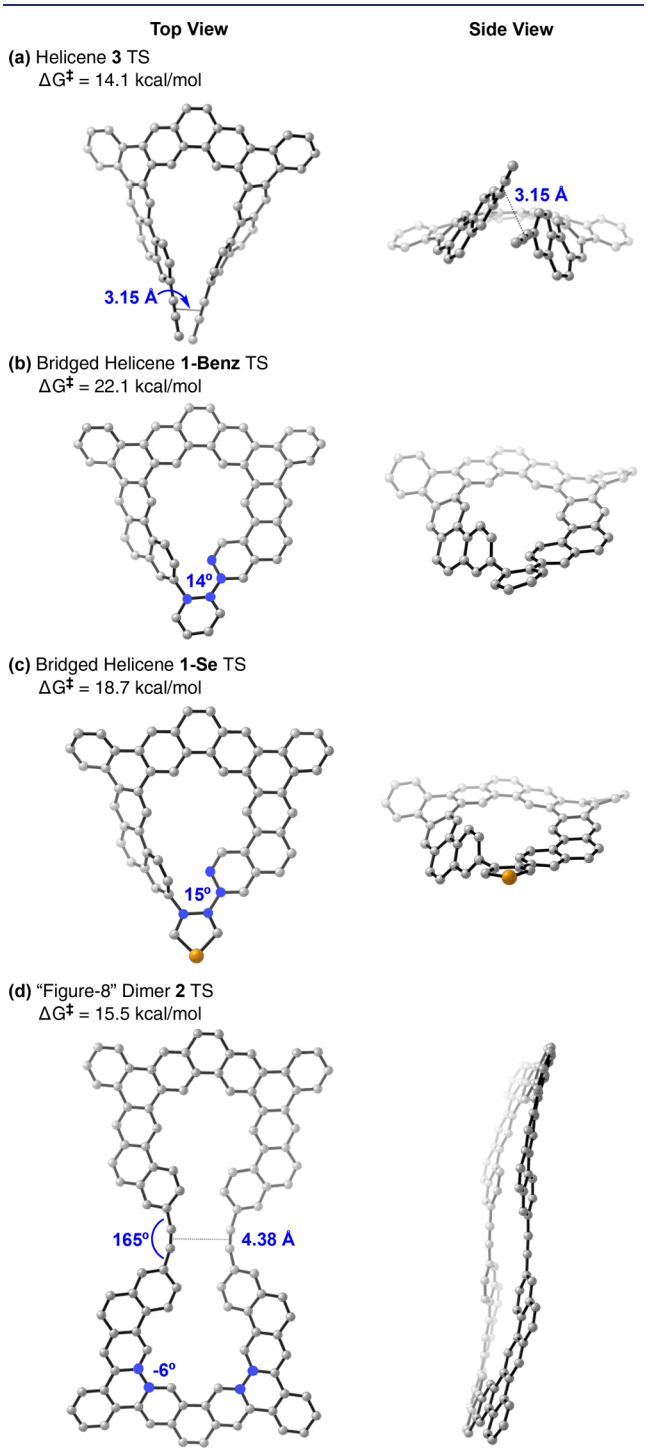

Figure 4. DFT-calculated (B3LYP-D3/6-31G(d)) enantiomerization transition states (TSs) and free energy barriers ($\Delta G^{\ddagger}$). Side chains and hydrogens are omitted for clarity.

where side chains and hydrogens have been omitted for clarity (see SI for full structures and details). The trend in calculated $\Delta G^{\ddagger}$ values is consistent with that observed experimentally. Remarkably, there is only a slight increase in calculated $\Delta G^{\ddagger}_{enant}$ for figure-eight **2** compared to its helicene precursor **3** (15.5 vs 14.1 kcal/mol). In stark contrast, the calculated $\Delta G^{\ddagger}_{enant}$ for the figure-eight dimer of [5]helicene (**D**, Figure

https://dx.doi.org/10.1021/jacs.0c03177
J. Am. Chem. Soc. 2020, 142, 11084−11091

1a) is more than two times that of monomeric [5]helicene (51.1 vs 24.1 kcal/mol).[22] The distortion of the alkynyl groups (C−C≡C angle of 165°) in the transition state for **2** suggests that the flexibility of this linkage plays a role in its configurational lability. The calculations suggest that compounds **2** and **3** undergo concerted mechanisms via transition states with pseudo-D_{2h} and -C_s symmetries, respectively. The structure of the former resembles that for figure-eight **D**[22] and that of the latter is ubiquitous for carbohelicenes.[23] Bridged helicenes **1-Benz** and **1-Se** invert handedness by a two-step mechanism, proceeding through a C_s-symmetric intermediate that is 4.4 and 9.9 kcal/mol higher in energy than their C_2 conformers, respectively (Figures S35 and S38, respectively). The depicted transition state in each case is that for the rate-limiting transformation from the C_2 to the C_s conformer.

CONCLUSION

In conclusion, the alkynylated expanded helicene **3** acts as a linchpin to two distinct chiral macrocyclic nanocarbons. The bridged helicene (**1**) provides a platform to increase expanded helicene configurational stability via a "covalent locking" strategy. The serendipitous resolution of the enantiomers of the figure-eight macrocycle (**2**) in the solid state hints at an alternative, non-covalent strategy to increase configurational stability. Here, it is the intricate network in the crystal structure that stabilizes the enantiomers of this otherwise highly flexible molecule. Studies of the enantiomerization mechanisms of **1**−**3** with DFT provided insight that should enable access to more stable analogues, especially given the scalability and potential modularity of the synthetic tools described above.

ASSOCIATED CONTENT

Supporting Information

The Supporting Information is available free of charge at https://pubs.acs.org/doi/10.1021/jacs.0c03177.

Experimental procedures, characterization data, and computational details, including Figures S1−S44 and Tables S1−S8 (PDF)

Crystallographic information file for **2** (CIF)

AUTHOR INFORMATION

Corresponding Author

T. Don Tilley − *Department of Chemistry, University of California, Berkeley, California 94720, United States;* orcid.org/0000-0002-6671-9099; Email: tdtilley@berkeley.edu

Authors

Gavin R. Kiel − *Department of Chemistry, University of California, Berkeley, California 94720, United States;* orcid.org/0000-0001-6449-8547

Katherine L. Bay − *Department of Chemistry and Biochemistry, University of California, Los Angeles, California 90095, United States;* orcid.org/0000-0002-9917-8188

Adrian E. Samkian − *Department of Chemistry, University of California, Berkeley, California 94720, United States*

Nathaniel J. Schuster − *Department of Chemistry, Columbia University, New York, New York 10027, United States*

Janice B. Lin − *Department of Chemistry and Biochemistry, University of California, Los Angeles, California 90095, United States;* orcid.org/0000-0002-9333-5760

Rex C. Handford − *Department of Chemistry, University of California, Berkeley, California 94720, United States;* orcid.org/0000-0002-3693-1697

Colin Nuckolls − *Department of Chemistry, Columbia University, New York, New York 10027, United States;* orcid.org/0000-0002-0384-5493

K. N. Houk − *Department of Chemistry and Biochemistry, University of California, Los Angeles, California 90095, United States;* orcid.org/0000-0002-8387-5261

Complete contact information is available at: https://pubs.acs.org/10.1021/jacs.0c03177

Notes

The authors declare no competing financial interest.

ACKNOWLEDGMENTS

This work was funded by the National Science Foundation under Grant No. CHE-1708210. Crystallographic analysis of compound **2** was performed at The Advanced Light Source, which is supported by the Director, Office of Science, Office of Basic Energy Sciences, of the U.S. Department of Energy under Contract No. DE-AC02-05CH11231. We thank UC Berkeley's NMR facility for resources provided and the staff for their assistance. Instruments in the NMR facility are supported in part by NIH S10OD024998. Computations were performed on the Hoffman2 cluster at UCLA and the Extreme Science and Engineering Discovery Environment (XSEDE), which is supported by the National Science Foundation (OCI-1053575). The CD spectra were measured at the Precision Biomolecular Characterization Facility (PBCF) at Columbia University. The PBCF was made possible by funding from the U.S. National Institutes of Health under award no. 1S10OD025102-01. We thank Dr. Jia Ma for his management of the PBCF, Stephen von Kugelgen and Felix R. Fischer for initial samples of EtC≡Mo(OC(CH$_3$)(CF$_3$)$_2$)$_3$(DME), and Stephen von Kugelgen and Harrison M. Bergman for helpful discussions.

REFERENCES

(1) (a) Rickhaus, M.; Mayor, M.; Juríček, M. Strain-Induced Helical Chirality in Polyaromatic Systems. *Chem. Soc. Rev.* **2016**, *45*, 1542−1556. (b) Shen, Y.; Chen, C.-F. Helicenes: Synthesis and Applications. *Chem. Rev.* **2012**, *112* (3), 1463−1535. (c) Gingras, M. One Hundred Years of Helicene Chemistry. Part 3: Applications and Properties of Carbohelicenes. *Chem. Soc. Rev.* **2013**, *42* (3), 1051−1095. (d) Fernández-García, J. M.; Evans, P. J.; Filippone, S.; Herranz, M. Á.; Martín, N. Chiral Molecular Carbon Nanostructures. *Acc. Chem. Res.* **2019**, *52* (6), 1565−1574. (e) Tanaka, H.; Inoue, Y.; Mori, T. Circularly Polarized Luminescence and Circular Dichroisms in Small Organic Molecules: Correlation between Excitation and Emission Dissymmetry Factors. *ChemPhotoChem.* **2018**, *2* (5), 386−402.

(2) Brandt, J. R.; Salerno, F.; Fuchter, M. J. The Added Value of Small-Molecule Chirality in Technological Applications. *Nat. Rev. Chem.* **2017**, *1*, 45.

(3) (a) Pascal, R. A. Twisted Acenes. *Chem. Rev.* **2006**, *106* (12), 4809−4819. (b) Rickhaus, M.; Mayor, M.; Juríček, M. Chirality in Curved Polyaromatic Systems. *Chem. Soc. Rev.* **2017**, *46* (6), 1643−1660. (c) Majewski, M. A.; Stępień, M. Bowls, Hoops, and Saddles: Synthetic Approaches to Curved Aromatic Molecules. *Angew. Chem., Int. Ed.* **2019**, *58* (1), 86−116.

(4) (a) Campbell, K.; Tykwinski, R. R. Chiral Carbon-Rich Macrocycles and Cyclophanes. In *Carbon-Rich Compounds*; Haley, M. M., Tykwinski, R. R., Eds.; Wiley-VCH Verlag GmbH & Co. KGaA: Weinheim, Germany, 2006; pp 229−294. DOI: 10.1002/

3527607994.ch6. (b) Stępień, M.; Sprutta, N.; Latos-Grażyński, L. Figure Eights, Möbius Bands, and More: Conformation and Aromaticity of Porphyrinoids. *Angew. Chem., Int. Ed.* **2011**, *50* (19), 4288−4340. (c) Senthilkumar, K.; Kondratowicz, M.; Lis, T.; Chmielewski, P. J.; Cybińska, J.; Zafra, J. L.; Casado, J.; Vives, T.; Crassous, J.; Favereau, L.; Stępien, M. Lemniscular [16]-Cycloparaphenylene: A Radially Conjugated Figure-Eight Aromatic Molecule. *J. Am. Chem. Soc.* **2019**, *141* (18), 7421−7427. (d) Ball, M.; Fowler, B.; Li, P.; Joyce, L. A.; Li, F.; Liu, T.; Paley, D.; Zhong, Y.; Li, H.; Xiao, S.; Ng, F.; Steigerwald, M. L.; Nuckolls, C. Chiral Conjugated Corrals. *J. Am. Chem. Soc.* **2015**, *137* (31), 9982−9987. (e) Sato, S.; Yoshii, A.; Takahashi, S.; Furumi, S.; Takeuchi, M.; Isobe, H. Chiral Intertwined Spirals and Magnetic Transition Dipole Moments Dictated by Cylinder Helicity. *Proc. Natl. Acad. Sci. U. S. A.* **2017**, *114* (50), 13097−13101. (f) Sun, Z.; Matsuno, T.; Isobe, H. Stereoisomerism and Structures of Rigid Cylindrical Cycloarylenes. *Bull. Chem. Soc. Jpn.* **2018**, *91* (6), 907−921. (g) Weiland, K. J.; Brandl, T.; Atz, K.; Prescimone, A.; Häussinger, D.; Šolomek, T.; Mayor, M. Mechanical Stabilization of Helical Chirality in a Macrocyclic Oligothiophene. *J. Am. Chem. Soc.* **2019**, *141* (5), 2104−2110.

(5) (a) Zhao, D.; Moore, J. S. Shape-Persistent Arylene Ethynylene Macrocycles: Syntheses and Supramolecular Chemistry. *Chem. Commun.* **2003**, 807−818. (b) Iyoda, M.; Yamakawa, J.; Rahman, M. J. Conjugated Macrocycles: Concepts and Applications. *Angew. Chem., Int. Ed.* **2011**, *50* (45), 10522−10553. (c) Sprafke, J. K.; Kondratuk, D. V.; Wykes, M.; Thompson, A. L.; Hoffmann, M.; Drevinskas, R.; Chen, W.-H.; Yong, C. K.; Kärnbratt, J.; Bullock, J. E.; Malfois, M.; Wasielewski, M. R.; Albinsson, B.; Herz, L. M.; Zigmantas, D.; Beljonne, D.; Anderson, H. L. Belt-Shaped π-Systems: Relating Geometry to Electronic Structure in a Six-Porphyrin Nanoring. *J. Am. Chem. Soc.* **2011**, *133* (43), 17262−17273. (d) Schneebeli, S. T.; Frasconi, M.; Liu, Z.; Wu, Y.; Gardner, D. M.; Strutt, N. L.; Cheng, C.; Carmieli, R.; Wasielewski, M. R.; Stoddart, J. F. Electron Sharing and Anion−π Recognition in Molecular Triangular Prisms. *Angew. Chem., Int. Ed.* **2013**, *52* (49), 13100−13104. (e) Kayahara, E.; Kouyama, T.; Kato, T.; Takaya, H.; Yasuda, N.; Yamago, S. Isolation and Characterization of the Cycloparaphenylene Radical Cation and Dication. *Angew. Chem., Int. Ed.* **2013**, *52* (51), 13722−13726. (f) Golder, M. R.; Jasti, R. Syntheses of the Smallest Carbon Nanohoops and the Emergence of Unique Physical Phenomena. *Acc. Chem. Res.* **2015**, *48* (3), 557−566. (g) Ball, M.; Zhong, Y.; Fowler, B.; Zhang, B.; Li, P.; Etkin, G.; Paley, D. W.; Decatur, J.; Dalsania, A. K.; Li, H.; Xiao, S.; Ng, F.; Steigerwald, M. L.; Nuckolls, C. Macrocyclization in the Design of Organic N-Type Electronic Materials. *J. Am. Chem. Soc.* **2016**, *138* (39), 12861−12867. (h) Liu, C.; Sandoval-Salinas, M. E.; Hong, Y.; Gopalakrishna, T. Y.; Phan, H.; Aratani, N.; Herng, T. S.; Ding, J.; Yamada, H.; Kim, D.; Casanova, D.; Wu, J. Macrocyclic Polyradicaloids with Unusual Super-Ring Structure and Global Aromaticity. *Chem.* **2018**, *4* (7), 1586−1595.

(6) Reviews: (a) Li, C.; Yang, Y.; Miao, Q. Recent Progress in Chemistry of Multiple Helicenes. *Chem. - Asian J.* **2018**, *13* (8), 884−894. (b) Ball, M.; Zhong, Y.; Wu, Y.; Schenck, C.; Ng, F.; Steigerwald, M.; Xiao, S.; Nuckolls, C. Contorted Polycyclic Aromatics. *Acc. Chem. Res.* **2015**, *48* (2), 267−276. Selected examples: (c) Barnett, L.; Ho, D. M.; Baldridge, K. K.; Pascal, R. A. The Structure of Hexabenzotriphenylene and the Problem of Overcrowded "D_{3h}" Polycyclic Aromatic Compounds. *J. Am. Chem. Soc.* **1999**, *121* (4), 727−733. (d) Kang, S. J.; Ahn, S.; Kim, J. B.; Schenck, C.; Hiszpanski, A. M.; Oh, S.; Schiros, T.; Loo, Y.-L.; Nuckolls, C. Using Self-Organization To Control Morphology in Molecular Photovoltaics. *J. Am. Chem. Soc.* **2013**, *135* (6), 2207−2212. (e) Fujikawa, T.; Segawa, Y.; Itami, K. Synthesis, Structures, and Properties of π-Extended Double Helicene: A Combination of Planar and Nonplanar π-Systems. *J. Am. Chem. Soc.* **2015**, *137* (24), 7763−7768. (f) Wang, X.-Y.; Wang, X.-C.; Narita, A.; Wagner, M.; Cao, X.-Y.; Feng, X.; Müllen, K. Synthesis, Structure, and Chiroptical Properties of a Double [7]Heterohelicene. *J. Am. Chem. Soc.* **2016**, *138* (39), 12783−12786. (g) Pradhan, A.; Dechambenoit, P.; Bock, H.; Durola, F. Fused Helicene Chains: Towards Twisted Graphene Nanoribbons. *Chem. - Eur. J.* **2016**, *22* (50), 18227−18235. (h) Hu, Y.; Wang, X.-Y.; Peng, P.-X.; Wang, X.-C.; Cao, X.-Y.; Feng, X.; Müllen, K.; Narita, A. Benzo-Fused Double [7]Carbohelicene: Synthesis, Structures, and Physicochemical Properties. *Angew. Chem., Int. Ed.* **2017**, *56* (12), 3374−3378. (i) Hosokawa, T.; Takahashi, Y.; Matsushima, T.; Watanabe, S.; Kikkawa, S.; Azumaya, I.; Tsurusaki, A.; Kamikawa, K. Synthesis, Structures, and Properties of Hexapole Helicenes: Assembling Six [5]Helicene Substructures into Highly Twisted Aromatic Systems. *J. Am. Chem. Soc.* **2017**, *139* (51), 18512−18521.

(7) (a) Schaack, C.; Arrico, L.; Sidler, E.; Górecki, M.; Di Bari, L.; Diederich, F. Helicene Monomers and Dimers: Chiral Chromophores Featuring Strong Circularly Polarized Luminescence. *Chem. - Eur. J.* **2019**, *25* (34), 8003−8007. (b) Amemiya, R.; Mizutani, M.; Yamaguchi, M. Two-Component Gel Formation by Pseudoenantiomeric Ethynylhelicene Oligomers. *Angew. Chem., Int. Ed.* **2010**, *49* (11), 1995−1999. (c) Saiki, Y.; Sugiura, H.; Nakamura, K.; Yamaguchi, M.; Hoshi, T.; Anzai, J. [3 + 3]Cycloalkyne Dimers Linked by an Azo Group: A Stable Cis-Azo Compound Forms Polymeric Aggregates by Nonplanar $\pi-\pi$ Interactions. *J. Am. Chem. Soc.* **2003**, *125* (31), 9268−9269. (d) Thulin, B.; Wennerstrom, O. Propellicene or Bi-2,13-Pentahelicenylene. *Acta Chem. Scand.* **1976**, *30*, 688−690. (e) Robert, A.; Dechambenoit, P.; Hillard, E. A.; Bock, H.; Durola, F. Non-Planar Oligoarylene Macrocycles from Biphenyl. *Chem. Commun.* **2017**, *53* (84), 11540−11543. (f) Ushiyama, A.; Hiroto, S.; Yuasa, J.; Kawai, T.; Shinokubo, H. Synthesis of a Figure-Eight Azahelicene Dimer with High Emission and CPL Properties. *Org. Chem. Front.* **2017**, *4* (5), 664−667. (g) Nakanishi, W.; Matsuno, T.; Ichikawa, J.; Isobe, H. Illusory Molecular Expression of "Penrose Stairs" by an Aromatic Hydrocarbon. *Angew. Chem., Int. Ed.* **2011**, *50* (27), 6048−6051. (h) Naulet, G.; Sturm, L.; Robert, A.; Dechambenoit, P.; Röhricht, F.; Herges, R.; Bock, H.; Durola, F. Cyclic Tris-[5]Helicenes with Single and Triple Twisted Möbius Topologies and Möbius Aromaticity. *Chem. Sci.* **2018**, *9* (48), 8930−8936. (i) Jiang, X.; Laffoon, S. D.; Chen, D.; Pérez-Estrada, S.; Danis, A. S.; Rodríguez-López, J.; Garcia-Garibay, M. A.; Zhu, J.; Moore, J. S. Kinetic Control in the Synthesis of a Möbius Tris((Ethynyl)[5]Helicene) Macrocycle Using Alkyne Metathesis. *J. Am. Chem. Soc.* **2020**, *142* (14), 6493−6498. (j) Fox, J. M.; Lin, D.; Itagaki, Y.; Fujita, T. Synthesis of Conjugated Helical Acetylene-Bridged Polymers and Cyclophanes. *J. Org. Chem.* **1998**, *63* (6), 2031−2038.

(8) Kiel, G. R.; Patel, S. C.; Smith, P. W.; Levine, D. S.; Tilley, T. D. Expanded Helicenes: A General Synthetic Strategy and Remarkable Supramolecular and Solid-State Behavior. *J. Am. Chem. Soc.* **2017**, *139* (51), 18456−18459.

(9) Nakakuki, Y.; Hirose, T.; Matsuda, K. Synthesis of a Helical Analogue of Kekulene: A Flexible π-Expanded Helicene with Large Helical Diameter Acting as a Soft Molecular Spring. *J. Am. Chem. Soc.* **2018**, *140* (45), 15461−15469.

(10) Kiel, G. R.; Bergman, H. M.; Tilley, T. D. Site-Selective [2+2 + n] Cycloadditions for Rapid, Scalable Access to Alkynylated Polycyclic Aromatic Hydrocarbons. *Chem. Sci.* **2020**, *11*, 3028−3035.

(11) Kezuka, S.; Tanaka, S.; Ohe, T.; Nakaya, Y.; Takeuchi, R. Iridium Complex-Catalyzed [2+2+2] Cycloaddition of α,ω-Diynes with Monoynes and Monoenes. *J. Org. Chem.* **2006**, *71* (2), 543−552.

(12) (a) During the course of our work, Tanaka reported a synthetic strategy to access a [6]cycloparaphenylene derivative using an analogous, Rh-catalyzed [2+2+2] macrocyclization. See: Hayase, N.; Sugiyama, H.; Uekusa, H.; Shibata, Y.; Tanaka, K. Rhodium-Catalyzed Synthesis, Crystal Structures, and Photophysical Properties of [6]Cycloparaphenylene Tetracarboxylates. *Org. Lett.* **2019**, *21* (11), 3895−3899. (b) "Bridging" strategies to influence the conformational behavior of helicenes appear to be rare, but they are not unprecedented. For example, Marinetti and co-workers showed that bridging the termini of [5]helicene with a chiral tether can influence the equilibrium between *P* and *M* configurations. See: El Abed, R.; Ben Hassine, B.; Genet, J.-P.; Gorsane, M.; Madec, J.; Ricard, L.;

https://dx.doi.org/10.1021/jacs.0c03177
J. Am. Chem. Soc. 2020, 142, 11084−11091

Marinetti, A. Synthesis of a Configurationally Locked [5]Helicene Derivative. *Synthesis* **2004**, *2004* (15), 2513−2516.
(13) (a) Rosenthal, U.; Ohff, A.; Baumann, W.; Tillack, A.; Görls, H.; Burlakov, V. V.; Shur, V. B. Struktur, Eigenschaften und NMR-spektroskopische Charakterisierung von $Cp_2Zr(Pyridin)(Me_3SiC{\equiv}CSiMe_3)$. *Z. Anorg. Allg. Chem.* **1995**, *621* (1), 77−83. (b) Nitschke, J. R.; Zürcher, S.; Tilley, T. D. New Zirconocene-Coupling Route to Large, Functionalized Macrocycles. *J. Am. Chem. Soc.* **2000**, *122* (42), 10345−10352.
(14) Takahashi, T.; Xi, Z.; Yamazaki, A.; Liu, Y.; Nakajima, K.; Kotora, M. Cycloaddition Reaction of Zirconacyclopentadienes to Alkynes: Highly Selective Formation of Benzene Derivatives from Three Different Alkynes. *J. Am. Chem. Soc.* **1998**, *120* (8), 1672−1680.
(15) (a) Fagan, P. J.; Nugent, W. A.; Calabrese, J. C. Metallacycle Transfer from Zirconium to Main Group Elements: A Versatile Synthesis of Heterocycles. *J. Am. Chem. Soc.* **1994**, *116* (5), 1880−1889. (b) Takahashi, T.; Hara, R.; Nishihara, Y.; Kotora, M. Copper-Mediated Coupling of Zirconacyclopentadienes with Dihalo Aromatic Compounds. Formation of Fused Aromatic Rings. *J. Am. Chem. Soc.* **1996**, *118* (21), 5154−5155. (c) Takahashi, T.; Li, Y.; Stepnicka, P.; Kitamura, M.; Liu, Y.; Nakajima, K.; Kotora, M. Coupling Reaction of Zirconacyclopentadienes with Dihalonaphthalenes and Dihalopyridines: A New Procedure for the Preparation of Substituted Anthracenes, Quinolines, and Isoquinolines. *J. Am. Chem. Soc.* **2002**, *124* (4), 576−582. (d) Yan, X.; Xi, C. Conversion of Zirconacyclopentadienes into Metalloles: Fagan−Nugent Reaction and Beyond. *Acc. Chem. Res.* **2015**, *48* (4), 935−946.
(16) (a) Ge, P.-H.; Fu, W.; Herrmann, W. A.; Herdtweck, E.; Campana, C.; Adams, R. D.; Bunz, U. H. F. Structural Characterization of a Cyclohexameric Meta-Phenyleneethynylene Made by Alkyne Metathesis with In Situ. *Angew. Chem., Int. Ed.* **2000**, *39* (20), 3607−3610. (b) Miljanić, O. Š.; Vollhardt, K. P. C.; Whitener, G. D. An Alkyne Metathesis-Based Route to Ortho-Dehydrobenzannulenes. *Synlett* **2003**, *34*, 29−34. (c) Zhang, W.; Moore, J. S. Reaction Pathways Leading to Arylene Ethynylene Macrocycles via Alkyne Metathesis. *J. Am. Chem. Soc.* **2005**, *127* (33), 11863−11870. (d) Yu, C.; Jin, Y.; Zhang, W. Shape-Persistent Macrocycles through Dynamic Covalent Reactions. In *Dynamic Covalent Chemistry*; John Wiley & Sons, Ltd., 2017; pp 121−163. DOI: 10.1002/9781119075738.ch3.
(17) Gdula, R. L.; Johnson, M. J. A. Highly Active Molybdenum−Alkylidyne Catalysts for Alkyne Metathesis: Synthesis from the Nitrides by Metathesis with Alkynes. *J. Am. Chem. Soc.* **2006**, *128* (30), 9614−9615.
(18) Heppekausen, J.; Stade, R.; Goddard, R.; Fürstner, A. Practical New Silyloxy-Based Alkyne Metathesis Catalysts with Optimized Activity and Selectivity Profiles. *J. Am. Chem. Soc.* **2010**, *132* (32), 11045−11057.
(19) The depicted structure contains molecules with *PP* configuration, and a Flack parameter of 0.0(4) suggests that this is the correct absolute configuration for the analyzed crystal; however, the large standard uncertainty precludes definitive conclusions from being drawn. In addition, while it is highly likely that these crystals formed as conglomerates (since there was no external chiral bias), this has not been experimentally evaluated.
(20) Spek, A. L. PLATON SQUEEZE: A Tool for the Calculation of the Disordered Solvent Contribution to the Calculated Structure Factors. *Acta Crystallogr., Sect. C: Struct. Chem.* **2015**, *71* (1), 9−18.
(21) Rieger, R.; Müllen, K. Forever Young: Polycyclic Aromatic Hydrocarbons as Model Cases for Structural and Optical Studies. *J. Phys. Org. Chem.* **2010**, *23* (4), 315−325.
(22) Robert, A.; Naulet, G.; Bock, H.; Vanthuyne, N.; Jean, M.; Giorgi, M.; Carissan, Y.; Aroulanda, C.; Scalabre, A.; Pouget, E.; Durola, F.; Coquerel, Y. Cyclobishelicenes: Shape-Persistent Figure-Eight Aromatic Molecules with Promising Chiroptical Properties. *Chem. - Eur. J.* **2019**, *25*, 14364−14369.
(23) (a) Janke, R. H.; Haufe, G.; Würthwein, E.-U.; Borkent, J. H. Racemization Barriers of Helicenes: A Computational Study. *J. Am. Chem. Soc.* **1996**, *118* (25), 6031−6035. (b) Barroso, J.; Cabellos, J. L.; Pan, S.; Murillo, F.; Zarate, X.; Fernandez-Herrera, M. A.; Merino, G. Revisiting the Racemization Mechanism of Helicenes. *Chem. Commun.* **2018**, *54* (2), 188−191.

https://dx.doi.org/10.1021/jacs.0c03177
J. Am. Chem. Soc. 2020, 142, 11084−11091